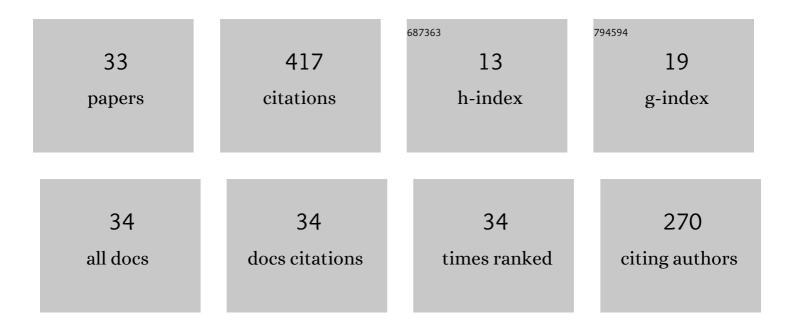
Toshiki Watanabe

List of Publications by Year in descending order

Source: https://exaly.com/author-pdf/9579723/publications.pdf Version: 2024-02-01



#	Article	IF	CITATIONS
1	Understanding the reaction mechanism and performances of 3d transition metal cathodes for all-solid-state fluoride ion batteries. Journal of Materials Chemistry A, 2021, 9, 406-412.	10.3	33
2	High Ionic Conductivity of Liquid-Phase-Synthesized Li ₃ PS ₄ Solid Electrolyte, Comparable to That Obtained via Ball Milling. ACS Applied Energy Materials, 2021, 4, 2275-2281.	5.1	33
3	Investigation of the Suppression of Dendritic Lithium Growth with a Lithium-Iodide-Containing Solid Electrolyte. Chemistry of Materials, 2021, 33, 4907-4914.	6.7	30
4	Nanoscale in situ observations of crack initiation and propagation in carbon fiber/epoxy composites using synchrotron radiation X-ray computed tomography. Composites Science and Technology, 2020, 197, 108244.	7.8	29
5	Nanoscopic origin of cracks in carbon fibre-reinforced plastic composites. Scientific Reports, 2019, 9, 19300.	3.3	27
6	Phase Transition Behavior of MgMn ₂ O ₄ Spinel Oxide Cathode during Magnesium Ion Insertion. Chemistry of Materials, 2021, 33, 1006-1012.	6.7	24
7	Reversible and Fast (De)fluorination of Highâ€Capacity Cu ₂ O Cathode: One Step Toward Practically Applicable Allâ€Solidâ€State Fluorideâ€lon Battery. Advanced Energy Materials, 2021, 11, 2102285.	19.5	23
8	Synthesis of Sulfide Solid Electrolytes through the Liquid Phase: Optimization of the Preparation Conditions. ACS Omega, 2020, 5, 26287-26294.	3.5	22
9	Effect of Interaction among Magnesium Ions, Anion, and Solvent on Kinetics of the Magnesium Deposition Process. Journal of Physical Chemistry C, 2020, 124, 28510-28519.	3.1	19
10	Cu–Pb Nanocomposite Cathode Material toward Room-Temperature Cycling for All-Solid-State Fluoride-Ion Batteries. ACS Applied Energy Materials, 2021, 4, 3352-3357.	5.1	18
11	Kinetic analysis and alloy designs for metal/metal fluorides toward high rate capability for all-solid-state fluoride-ion batteries. Journal of Materials Chemistry A, 2021, 9, 7018-7024.	10.3	16
12	<i>Operando</i> X-ray Absorption Spectroscopic Study on the Influence of Specific Adsorption of the Sulfo Group in the Perfluorosulfonic Acid Ionomer on the Oxygen Reduction Reaction Activity of the Pt/C Catalyst. ACS Applied Energy Materials, 2021, 4, 1143-1149.	5.1	15
13	Studies on the inhibition of lithium dendrite formation in sulfide solid electrolytes doped with LiX (XÂ=ÂBr, I). Solid State Ionics, 2022, 377, 115869.	2.7	15
14	High Rate Capability from a Graphite Anode through Surface Modification with Lithium Iodide for All-Solid-State Batteries. ACS Applied Energy Materials, 2022, 5, 667-673.	5.1	15
15	Rate-Determining Process at Electrode/Electrolyte Interfaces for All-Solid-State Fluoride-Ion Batteries. ACS Applied Materials & Interfaces, 2021, 13, 30198-30204.	8.0	14
16	Anion Substitution at Apical Sites of Ruddlesden–Popper-type Cathodes toward High Power Density for All-Solid-State Fluoride-Ion Batteries. Chemistry of Materials, 2022, 34, 609-616.	6.7	13
17	<i>Operando</i> soft X-ray absorption spectroscopic study on microporous carbon-supported sulfur cathodes. RSC Advances, 2020, 10, 39875-39880.	3.6	8
18	Nanoscale in situ observation of damage formation in carbon fiber/epoxy composites under mixed-mode loading using synchrotron radiation X-ray computed tomography. Composites Science and Technology, 2022, 230, 109332.	7.8	8

Τοςμικι Watanabe

#	Article	IF	CITATIONS
19	3D Spectromicroscopic Observation of Yb-Silicate Ceramics Using XAFS-CT. Microscopy and Microanalysis, 2018, 24, 484-485.	0.4	6
20	Impact of the Composition of Alcohol/Water Dispersion on the Proton Transport and Morphology of Cast Perfluorinated Sulfonic Acid Ionomer Thin Films. ACS Omega, 2021, 6, 14130-14137.	3.5	6
21	Quantitative Evaluation of the Activity of Low-Spin Tetravalent Nickel Ion Sites for the Oxygen Evolution Reaction. ACS Applied Energy Materials, 2021, 4, 10731-10738.	5.1	5
22	Quadruple perovskite oxides CaMn7O12 proceed by twoâ€activeâ€site reaction mechanism for oxygen evolution reaction. ChemElectroChem, 0, , .	3.4	5
23	Development of spectromicroscopes for multiscale observation of heterogeneity in materials at photon factory, IMSS, KEK. AIP Conference Proceedings, 2019, , .	0.4	4
24	Substrate-dependent proton transport and nanostructural orientation of perfluorosulfonic acid polymer thin films on Pt and carbon substrate. Solid State Ionics, 2020, 357, 115456.	2.7	4
25	<i>Operando</i> X-ray Absorption Spectroscopic Study on the Effect of Ionic Liquid Coverage upon the Oxygen Reduction Reaction Activity of Pd-core Pt-shell Catalysts. Electrochemistry, 2021, 89, 31-35.	1.4	4
26	The Effect of Cation Mixing in LiNiO 2 toward the Oxygen Evolution Reaction. ChemElectroChem, 2021, 8, 70-76.	3.4	4
27	State of the Active Site in La _{1–<i>x</i>} Sr _{<i>x</i>} CoO _{3â~î^} Under Oxygen Evolution Reaction Investigated by Total-Reflection Fluorescence X-Ray Absorption Spectroscopy. ACS Applied Energy Materials, 2022, 5, 4108-4116.	5.1	4
28	Development of dispersive XAFS system for analysis of time-resolved spatial distribution of electrode reaction. Journal of Synchrotron Radiation, 2015, 22, 1227-1232.	2.4	3
29	Finding Degradation Trigger Sites of Structural Materials for Airplanes Using Xâ€Ray Microscopy. Chemical Record, 2019, 19, 1462-1468.	5.8	3
30	Development of in situ cell for simultaneous XAFS/XRD measurements at high temperatures. Radiation Physics and Chemistry, 2020, 175, 108153.	2.8	3
31	Stability of Copper Nitride Nanoparticles under High Humidity and in Solutions with Different Acidity. Chemistry Letters, 2015, 44, 755-757.	1.3	2
32	In situ XRM Observation of Cracking in CFRP during Nanomechanical Testing. Microscopy and Microanalysis, 2018, 24, 432-433.	0.4	2
33	Nanoscale crack initiation and propagation in carbon fiber/epoxy composites using synchrotron: 3D image data. Data in Brief, 2020, 31, 105894.	1.0	0